Multi-Algorithm Artifact Correction (MAAC) Procedure Part One: Algorithm and Example

Joseph Dien

Department of Human Development and Quantitative Methodology, University of Maryland, 3304 Benjamin Building, College Park, MD 20742, USA.

Short Title: MAAC

Dien, J. (2024). Multi-Algorithm Artifact Correction (MAAC) Procedure Part One: Algorithm and Example. Biological Psychology, 108775. (DOI: https://doi.org/10.1016/j.biopsycho.2024.108775)

Address for correspondence: Joseph Dien, Department of Human Development and Quantitative Methodology, University of Maryland, 3304 Benjamin Building, College Park, MD 20742, USA.

Phone: 202-297-8117. E-mail: jdien07@mac.com. URL: http://joedien.com.

Abstract

The Multi-Algorithm Artifact Correction (MAAC) procedure is presented for electroencephalographic (EEG) data, as made freely available in the open-source EP Toolkit (Dien, 2010). First the major EEG artifact correction methods (regression, spatial filters, principal components analysis, and independent components analysis) are reviewed. Contrary to the dominant approach of picking one method that is thought to be most effective, this review concludes that none are globally superior, but rather each has strengths and weaknesses. Then each of the major artifact types are reviewed (Blink, Corneo-Retinal Dipole, Saccadic Spike Potential, and Movement). For each one, it is proposed that one of the major correction methods is best matched to address it, resulting in the MAAC procedure. The MAAC itself is then presented, as implemented in the EP Toolkit, in order to provide a sense of the user experience. The primary goal of this present paper is to make the conceptual argument for the MAAC approach.

Key Terms: ERP, EEG, artifact, statistics, open-source software

1.0 General Introduction

An issue that every electroencephalography (EEG) researcher faces is that while this method is exquisitely sensitive to microvolt level brain signals, it is also equally sensitive to noise. Noise can be defined as being any electrical signal that the researcher is not interested in, whether it be brain activity unrelated to the experimental questions or artifactual signals that arise outside the brain, as from the physical movements of the eyes. Traditionally, this noise is mitigated in the time-domain (event-related potentials or ERPs) by averaging over trials and in the frequency-domain by excluding activity outside the frequencies of interest.

Large amplitude noise that is not sufficiently contained by these strategies must then be addressed by other methods (Anderer et al., 1999; Fatourechi et al., 2007). The simplest and oldest is simply to reject time periods that are contaminated by large amplitude noise. There are several drawbacks to such an approach. The first is that it reduces the amount of data available for analysis. The second is that discarding such data may produce confounds, both within-participant if the noise (e.g., eye blinks) is greater in some conditions than others (e.g., due to task difficulty) and between-participant if the noise is greater in some groups (e.g., patients suffering from schizophrenia). The third is that some noise is relatively subtle or pervasive (e.g., saccade-related noise) and therefore not readily excluded.

Another approach, for noise due to behaviors under volitional control (e.g., blinking), is to request that the participants suppress the behavior during the task period. This strategy also has its drawbacks. First, such an instruction can induce a cognitive load, and in the case of blinking has been shown to reduce auditory N1 and both auditory and visual P300 amplitudes (Ochoa & Polich, 2000; Verleger, 1991). Second, it can simply cause the artifact to be less

detectable. For example, if participants are asked only to blink during inter-trial intervals, doing so can result in the blink recovery artifact (Klein & Skrandies, 2013) contaminating the baseline period.

For all these reasons, many if not most research groups use artifact correction methods of various types. Ongoing progress in statistical and signal processing methods have driven increasing interest in the development of better methods. While a number of software packages are now available and in widespread use, most rely on a single algorithm to address all types of artifacts, with independent components analysis currently attracting the most attention. While there are many existing algorithm-centered reports that seek to identify the best algorithm for dealing with artifacts broadly defined (e.g., Kirkove et al., 2014), this current report adopts an artifact-centered approach in which the correction procedure is designed around specific artifacts and their characteristics. The present report makes the argument that trying to identify a single algorithm that best solves all types of artifacts is an ill-posed question (Urigüen & Garcia-Zapirain, 2015). Each algorithm is a tool that will work best when it is matched to the unique characteristics of a noise source. This report therefore presents the Multi-Algorithm Artifact Correction or MAAC procedure, wherein each stage utilizes a different algorithm that is tailored to address a specific noise source.

We will first review the major artifact correction algorithms, each of which is used in some stage of the MAAC, to explain why it is being used and so a potential user could understand what is happening. Then we will review the major artifact types so that we can make the argument for why each is best addressed by a different algorithm and so that again a potential user can understand how to use it in the context of the MAAC. Finally, we will provide a graphical example of how the MAAC is applied in the context of the EP Toolkit (Dien, 2010b), which stands for ERP PCA Toolkit, which in turn stands for Event-related Potential Principal

Components Analysis Toolkit (although its scope has since extended beyond its original focus on PCA). Companion papers will provide the empirical evaluation of the MAAC design choices (Dien et al., 2024) and how it fares against competing methods (Dien & O'Hare, 2024).

Glossary

CRD	corneo-retinal dipole
EEG	electroencephalography
EMCP	eye movement correction program
EMG	electromyographic
EOG	electrooculographic
ERP	event-related potential
HEOG	horizontal electrooculographic
ICA	independent components analysis
MAAC	multi-algorithm artifact correction
PCA	principal components analysis
SP	spike potential
VEOG	vertical electrooculographic

1.1 Artifact Correction Algorithms

The major extant algorithms are based on regression, spatial filters, principal components analysis (PCA), and independent components analysis (ICA). In regression, typically some kind of measure, such as a linear combination of electrooculographic (EOG) channels (Ifeachor et al., 1988), is used as an estimate of the artifact (Brunia et al., 1989; Croft & Barry, 2000; Elbert et al., 1985; Gratton et al., 1983; Jervis et al., 1988; Semlitsch et al., 1986). A regression procedure is then carried out with the EEG channels to try to determine

what portion of a given EEG channel is comprised of the artifact and then it is subtracted. A general challenge of this approach is obtaining a pure measure of the artifact, as otherwise this procedure will subtract out whatever portion of the signal contaminates the estimate of the artifact (Berg & Scherg, 1991). When EOG channels are used as the estimate of the artifact, the validity of subtracting out all the activity in the EOG channels, such that it results in flat lines, is questionable. Also, it has been reported that a substantial residual may be left afterwards (Berg, 1986).

A second approach is the spatial filter approach, also known as a vector filter (Gratton et al., 1989). In this method, a putative scalp topography of the artifact, described as a set of coefficients or propagation factors, is the starting point (Lins et al., 1993a). Its amplitude is then computed as some type of a weighted sum of the electrodes at a given time. In principle, it could also be applied in the temporal domain (where the variables are time points) as a set of coefficients that describe a canonical waveform. Although regression may be used to help generate the template, this approach differs from the first approach in that differential activity in the EOG channels is not assumed to be solely due to artifact. The spatial filter may then be further refined using source modeling, as in Multiple Source Eye Correction (Berg & Scherg, 1994; Lins et al., 1993b).

This approach has the advantage over the regression approach that the artifacts are defined more precisely, in terms of multiple channels. It has the disadvantage that it too can have difficulty preserving real brain signals. In general, the amplitude of a spatial filter measure is a function of both the similarity of the signal and the amplitude of the signal, so a moderate similar signal or a large non-similar signal can both produce a substantial fit to the filter, resulting in some of the signal being subtracted (Ille et al., 2002). This template approach will be less sensitive to activity at the EOG sites but will be susceptible to activity at other sites.

A third approach is PCA (Gorsuch, 1983). Typically the data are recharacterized as a new set of linear combinations of the variables such that each one in turn represents the maximal degree of variance not already accounted for. These factors (normally termed "components" but this can cause confusion in the context of ERPs) are then rotated to a mathematically equivalent but more interpretable solution (ideally where each factor reflects only one signal). While PCA is often criticized in the EEG literature for producing orthogonal (uncorrelated) factors, this is only the case if an orthogonal rotation like Varimax (Kaiser, 1958) is utilized. Oblique rotations like Promax (Hendrickson & White, 1964) allow for correlated factors and indeed yield substantially improve ERP results over Varimax (Dien, 2010a; Dien et al., 2003, 2005). While this method has seen widespread use in the analysis of ERP data (Chapman & McCrary, 1995; Dien, 2012; Dien & Frishkoff, 2005; Donchin, 1966), it has seen only limited evaluation for artifact correction (Kaczorowska et al., 2017; Lagerlund et al., 1997; Wallstrom et al., 2004) except as an initial preparatory step for some other method (Berg & Scherg, 1994).

The likely reason for this neglect is that PCA is poorly suited for blink correction, the focus of most of the methodological work. The reason is that typical rotations such as Varimax and Promax utilize rotational criteria that favor solutions where the loadings are either zero or have a large absolute amplitude (Gorsuch, 1983). When conventional multivariate statistical procedures are applied to EEG data, they can do so either in the spatial or the temporal domain (Dien, 1998). When the rotation is performed in the spatial domain (where the variables represent channels and the time points are the observations) as is typically done for blink correction, it is not an appropriate criterion since volume conduction ensures that factor loadings will be non-zero at nearly all the channels (Dien, 1998, 2010a). What has not been generally

recognized is that PCA is highly promising for artifact correction in the temporal domain, as will be described later in this report.

Finally, the fourth approach relies on independent components analysis or ICA (Hyvärinen et al., 2001; Onton et al., 2006). ICA differs from PCA in that it minimizes parameters known to be sensitive to the degree of mixing of separate signals. It essentially seeks to rotate the linear combinations of variables, factors (again avoiding the use of the term "components"), until they ideally each reflect the contribution of only one underlying signal. Whereas PCA arose from the statistics literature, ICA arose from the electrical engineering literature, resulting in different terminology for the same concepts (for translations, see Dien et al., 2007).

It is common to first perform an unrotated PCA on the data (i.e., sphering) as a short-cut towards achieving the solution (Hyvärinen et al., 2001, p. 160). If this initial PCA is truncated to a smaller number of factors (also termed "using a subspace"), then doing so can also minimize overlearning (Hyvärinen et al., 2001, p. 268), which is a situation where the variable to observation ratio is too small, resulting in over-sensitivity to high-frequency noise in the obtained factors. A truncated PCA can also address the case of a singular data matrix that otherwise causes the ICA to fail (Hyvärinen et al., 2001, p. 267), as in a spatial ICA of a mean mastoids referenced dataset where both mastoid channels are present (the two channels will be mirrors of each other and hence be redundant informationally). When an initial PCA is applied, ICA can be thought of as a PCA rotation with useful properties (Delorme & Makeig, 2004, p. 13; Hyvärinen et al., 2001, p. 268).

While there are many such rotations, perhaps the most commonly used ICA rotation in EEG research is Infomax (Bell & Sejnowski, 1995; Comon, 1994; Makeig et al., 1996). Infomax relies on two rotational criteria. The first is the normality of the factor, as the Central Limit

Theorem (Fischer, 2010) indicates that a reduction of mixing should decrease the normality of the factor. The second parameter is independence, which is orthogonality at not just the second order (seeking to achieve r=0 where y=rx) but also higher moments (e.g., r=0 where $y=rx^2$). Independence is an even stronger, and hence less realistic constraint, than the orthogonality imposed by PCA-Varimax. It is therefore deeply ironic that many reports cite the overly strong nature of the orthogonality constraint of PCA-Varimax as a weakness compared to ICA's independence constraint. Infomax works better than PCA-Varimax because the algorithm seeks to maximize independence between factors but does not require the full achievement of independence, hence allowing for correlated factors, as does PCA-Promax. In general, -Infomax provides the best ERP solutions in the spatial domain whereas PCA-Promax provides the best solutions in the temporal domain (Dien, 2010a; Dien et al., 2007).

To expand on this point (since there is a lot of confusion on this topic), having a stronger constraint can be a weakness, not a strength, if it is not realistic. In other words, looking for sparkly heffalumps in a forest is not going to make you a better hunter than simply looking for heffalumps, when in fact what you should be looking for is deer. Although to take this analogy further, PCA-Promax looks for deer, Infomax looks for bison, and PCA-Varimax looks for sparkly deer. So PCA-Promax works best in the forest (temporal), Infomax works best on the plains (spatial), and PCA-Varimax is worse than either as sparkly deer don't exist.

It may help to further explain that a chief source of confusion on this topic is the nomenclature. There is a difference between the colloquial meaning of the word "independence", which is what one wants when separating things, and the mathematical meaning of the word "independence", which is a label that has been chosen for a particular mathematical condition. Consider for example, the characteristics of feathers and flight in animals. Although these are two entirely separate characteristics (penguins have feathers but

not flight, while bats fly but have no feathers), the two features are correlated (most feathered animals fly). Lack of correlation or dependence is not required for two things to be separate, and indeed requiring them to be "orthogonal" or "independent" may distort the results and cause the procedure to fail (Dien et al., 2005).

It may also help to reconsider how to describe role of orthogonality and independence. PCA-Varimax rotates to maximize the variance of the squared loadings (Kaiser, 1958), with an overly strict constraint of orthogonality. PCA-Promax allows the rotations to further pursue this criterion by relaxing the overly strict constraint of orthogonality (Hendrickson & White, 1964). We don't say that it rotates toward orthogonality; this condition was already accomplished by the initial eigenvalue decomposition, but that alone was not enough (due to rotational indeterminacy, which is that there are many possible versions of the solution that are all orthogonal, hence the need to rotate to the desired version), and indeed strict orthogonality is a problem, hence the need to relax it. In the same way, it is somewhat confusing to say that Infomax "rotates toward independence", although unlike PCA-Varimax, both aspects are accomplished in a single operation (Bell & Sejnowski, 1995). Perhaps it would be clearer to say that it rotates toward non-normality, with a soft constraint of maximizing independence as much as possible. It doesn't actually reach independence (which would be a bad thing) and independence alone would not achieve the desired goal even if the brain signals were in fact independent (due to rotational indeterminacy).

Much less confusion would exist if we instead said that PCA-Promax rotates toward "arfness" and Infomax rotates toward "gopness", and arfness is what one expects to find in the temporal domain and gopness is what one expects to find in the spatial domain, when analyzing EEG data. As typically encountered in EEG data, regardless of whether the data matrix is organized spatially or temporally, the brain signals are neither "orthogonal" nor "independent",

so a rotation that requires the data to be either will fail (for an example, see Dien, 2010a). The goal for both PCA-Promax and Infomax is to match the level of orthogonality/independence in the real signals, no more, no less. PCA-Promax and Infomax both work better than PCA-Varimax because they are able to do so. Interested readers should consult appropriate sources for more information (Dien, 1998, 2012; Dien et al., 2007; Dien & Frishkoff, 2005; Gorsuch, 1983; Hyvärinen et al., 2001).

A large number of studies have reported that ICA is highly effective for removing artifacts from EEG data (Delorme et al., 2007; Dimigen, 2020; Gao et al., 2010; Ghaderi et al., 2014; Haumann et al., 2016; Jung et al., 1997, 2000; Keren et al., 2010; Kong et al., 2013; Mammone & Morabito, 2008; Plöchl et al., 2012; Shoker et al., 2005; Winkler et al., 2011; Zhou & Gotman, 2009). A drawback of ICA is that it typically requires a substantial number of observations in order to be effective. This therefore means that ICA typically needs to be applied in the spatial domain (i.e., the variables are the channels) and the number of possible ICA factors is therefore restricted to the number of channels. For a sparse montage system, such a spatial ICA may not have enough available factors to cleanly separate both the EEG signals and the artifacts (Castellanos & Makarov, 2006; LeVan et al., 2006) whereas denser montages may result in multiple artifact factors due in part to overfitting (Viola et al., 2009).

The Multi-Algorithm Artifact Correction (MAAC) procedure uses all four of these algorithms, each directed at a major EEG artifact type most appropriate for its strengths. This selective fitting of the strengths of each of the four algorithms to the characteristics of a specific artifact, rather than using a single algorithm as a generalized artifact correction method, is the primary novel contribution of this report; thus, while the MAAC also implements some other optional routines, they were always intended as adjuncts to some other procedure, so their use in the MAAC are not worthy of further discussion.. In this next section, each artifact type will be

presented in turn, along with MAAC's strategy for correcting it. The four artifacts (Figure 1) and their correction methods are: 1) Blink [ICA], 2) Corneo-Retinal Dipole [regression], 3) Saccadic Spike Potential [spatial filter], and 4) Movement [PCA].

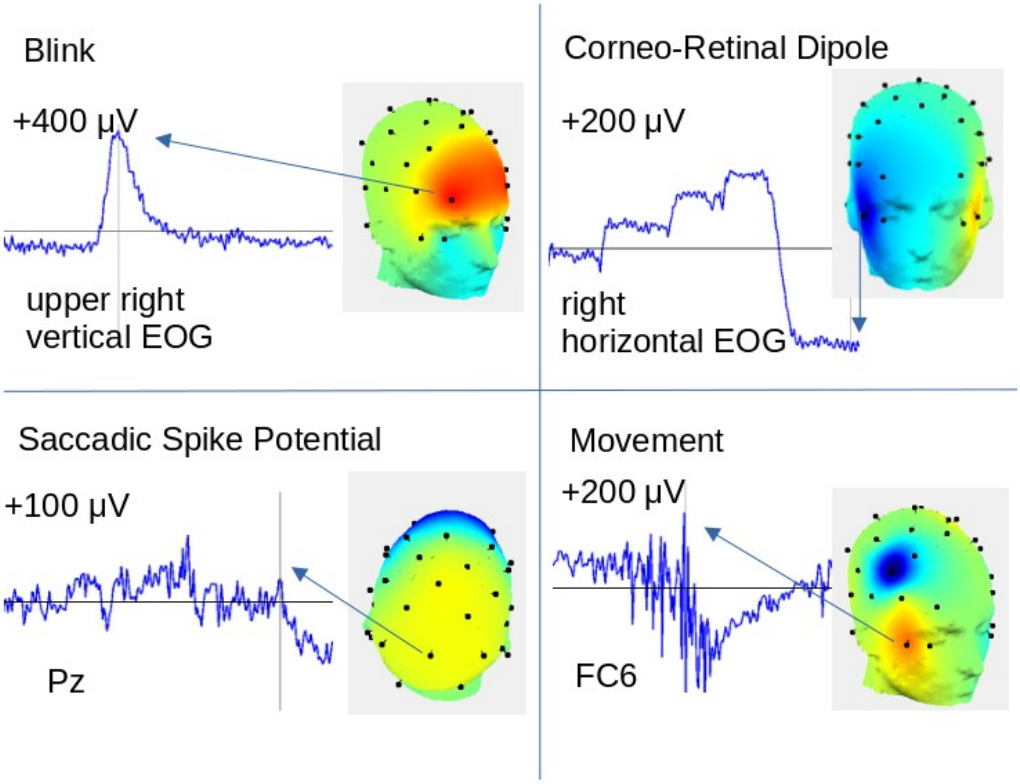

Figure 1 - Four Major Artifacts. Examples of all four major EEG artifacts discussed in this report. The maximum of the y-scale axis is indicated along with the channel. The arrow indicates the point in time from which the 3D head scalp topography was derived and which channel provided the waveform. The data are from the companion report (Dien et al., 2024).

1.2 Blink Artifact

The most troublesome artifact is the blink artifact. The descent of the upper eyelid over the eyeball appears to short the positively charged cornea to the forehead, producing a potential

field that is positive above the eye socket and negative below it (Matsuo et al., 1975; Picton et al., 2000b). This eyelid movement is accompanied by some eye rotation (Rottach et al., 1998), but this movement is not responsible for the bulk of the blink artifact (Iwasaki et al., 2005; Matsuo et al., 1975). Blinks are especially problematic for cognitive studies as they themselves are under cognitive control and indeed can serve as a psychophysiological measure (Brunyé & Gardony, 2017; Fogarty & Stern, 1989). They can therefore be not only large enough to swamp EEG activity of interest even far from the eye socket, their timing can also be event-related.

In recent years a consensus has developed that ICA is more effective for correcting eye-blinks (Ghaderi et al., 2014; Hoffmann & Falkenstein, 2008; Joyce et al., 2004; Jung et al., 2000). In general, the characteristics of the blink artifact seem to lend itself to ICA, namely its high amplitude, stationarity (i.e., invariance of its scalp topography), low normality of its distribution across the total session recording, and marked statistical independence from other EEG activity. For this reason, the MAAC also utilizes ICA for blink correction.

1.3 Corneo-Retinal Dipole

The second artifact to be corrected is the corneo-retinal dipole or CRD artifact. This effect arises from a stable potential difference between the cornea and the retina (Arden & Constable, 2006). Since the retina rests on a spherical surface, the non-radial vectors of the potential field cancel out outside of the eyeball, leaving just a radial component with the positive pole oriented towards the direction of gaze. This artifact is therefore best described as an eye direction artifact, although it is common in the literature to refer to it inaccurately as an "eye movement" artifact. This observation must be tempered to the extent that the amplifier is AC-coupled; the shorter the time constant, the more the recording will only reflect periods of change in the CRD (Peters, 1967). Typical time constants (e.g., 10 seconds from a typical amplifier

high-pass setting of .0159) of modern experiments are long enough to adequately characterize the CRD (e.g., with a high-pass setting of .0159, an eye movement every ten seconds would be sufficient to keep the amplitude of the recorded static CRD from more than halving). One scenario where it can be treated as being an eye-movement artifact is when the data are segmented and baseline-corrected; in this case, it will be subtracted out due to its presence in the baseline period and will only be noticeable when the participant changes eye-position mid-trial.

The distinction is important because it means that the artifact is always present even in the absence of eye movement, although if so it will only function as a confound when the gaze direction differs between conditions. An offset horizontal eye position can result in the appearance of frontal asymmetry. An offset vertical eye position results in potential fields with a topography that can mimic contingent negative variation components (Hillyard & Galambos, 1970). The amplitude of the CRD is positively correlated with illumination level and takes about thirty minutes to dark adapt (Fog, 1964), which consequently can also be a source of confound.

The most widely used method for the correction of the CRD artifact is a spatial filter algorithm, the Gratton eye movement correction program or EMCP (Coles & Gratton, 1989; Gratton et al., 1983). In this method, the uncorrected averaged ERP is first computed and then subtracted from the single-trial EEG and EOG channels to remove event-related activity. Regression analysis is then used to compute the propagation factors from the EOG channels to the EEG channels, separately for blink and non-blink periods (categorized by rate of change in the EOG channels). The most recent version of EMCP estimates the horizontal and vertical components of the CRD separately (Coles & Gratton, 1989). This results in an estimate of the blink and the CRD scalp topographies (Overton & Shagass, 1969). The blink activity and the CRD activity is then removed from the original uncorrected recordings, using either the blink or

the non-blink propagation factors depending on the categorization of the time points. This method was found to be a strong improvement over simple data rejection. It has the drawback of making the implicit assumption that all the activity in the EOG channels is artifactual, resulting in the removal of any EEG activity present in the EOG channels as well. Thus, the EOG channels are left flat and any EEG in these channels are removed not just from the EOG but also from the EEG channels matching the estimated blink and non-blink topographies (even if the EEG activity had a different scalp topography).

Concern over these issues has led to efforts to correct CRD artifact using some version of ICA (Gao et al., 2010; Ghaderi et al., 2014; Joyce et al., 2004; Kierkels et al., 2007; Mammone & Morabito, 2008; Mannan et al., 2016; Mennes et al., 2010; Plöchl et al., 2012; Sun et al., 2021; Winkler et al., 2011; Zeng et al., 2013; Zhou & Gotman, 2009). One issue with these efforts is that most of them did not distinguish between blink and CRD artifacts, making it hard to evaluate how well they did at the two respective types of artifacts. It is likely that an ICA method tuned for blink artifacts may not perform as well with CRD artifacts and vice versa (Gao et al., 2010). While it has been claimed that the scalp topography of blinks and CRD do not differ and can therefore be corrected with a single procedure (Croft & Barry, 2000; Schlögl et al., 2007), other investigations do not support this assertion (Berg & Scherg, 1991; Corby & Kopell, 1972; Picton et al., 2000b; Plöchl et al., 2012).

Perhaps the best prior study (Plöchl et al., 2012) presented a combination of EEG and eye-tracker data to argue that ICA, specifically Infomax, outperformed a regression-based procedure for both blinks and CRD artifact. While groundbreaking, this study had a number of limitations: 1) it only evaluated one ICA rotation, Infomax, 2) it only evaluated a relatively simple regression procedure, 3) while it provided strong proof-of-concept, it did not offer a routine ready for use by other EEG labs, especially the vast majority who lack eye-tracker equipment. We

argue that a well-tuned regression based method would outperform an automated ICA-based method that had to rely on criteria other than concurrent eye-tracker data because the CRD artifact is always present (favoring regression) and because the constraints of electrode dimensionality makes ICA prone to removing signal along with the CRD noise for non-high-density montages (they had 64 channels). Another such study (Sun et al., 2021) also reported good success with a Second-Order Blind Identification based method, but didn't provide the source code to replicate it or comparisons with any other methods.

For these reasons, the MAAC utilizes a regression procedure much like an improved Gratton EMCP. For one thing, rather than treating all of the EOG channel difference waves as being artifact to be removed, it takes the further step of estimating the CRD scalp topography and then only removing this estimated CRD activity, leaving the remainder of the EOG channel activity intact. It also does so for the entire recording instead of dividing it into distinct blink and saccade periods (since the CRD artifact is always present, even during blinks). A possible additional benefit of this latter refinement is that the resulting horizontal and vertical CRD estimates can then be used as a measure of gaze position (to the extent that overall head movement is controlled), although it has been reported to be less accurate for rapid movements (Hess et al., 1986).

1.4 Saccadic Spike Potential

The next is the spike potential or SP (Blinn, 1955; Brickett et al., 1984; Riggs et al., 1974). There is some dissension on whether to term this "presaccadic" or "saccadic", which is meaningful because the former would require it to be cortical rather than ocular in nature. We will follow the "saccadic" terminology because its onset timing relative to saccade initiation is difficult to determine (Keren et al., 2010), since eye-trackers suffer a lag before they register a

saccade, and it is neutral as to its source. This artifact starts at, or just before, the initiation of a saccade and takes the form of a positive pole over the parietal scalp and a negative pole that is oriented under the eyes that appears in published figures to have a peak latency of about ~10 ms after saccade initiation (Thickbroom & Mastaglia, 1985); some report (Boylan & Doig, 1988; Keren et al., 2010; Nativ et al., 1990; Plöchl et al., 2012; Riemslag et al., 1988) that it is then followed by a smaller reversed polarity spike and have termed them SPn and SPp respectively (Keren et al., 2010). Some researchers cite oculomyographic generators (Dimigen, 2020; Keren et al., 2010; Moster & Goldberg, 1990; Plöchl et al., 2012; Riemslag et al., 1988; Rodionov et al., 1996; Thickbroom & Mastaglia, 1985) based in part on source solutions in the eye socket region (Carl et al., 2012; Craddock et al., 2016; Hipp & Siegel, 2013; Picton et al., 2000a; Thickbroom & Mastaglia, 1985; Yuval-Greenberg et al., 2008); however, its overlap with the CRD artifact make it uncertain to what degree this location might be due to contamination from the the CRD (Riemslag et al., 1988). Additionally they point towards a report that a right hemispherectomy patient did not display asymmetry in the SP scalp topography (Thickbroom & Mastaglia, 1985), but this observation does not rule out a left hemisphere midline source.

In contrast, other researchers (Balaban & Weinstein, 1985; Csibra et al., 1997; Kurtzberg & Vaughan, 1982; Nativ et al., 1990; Parks & Corballis, 2008; Richards, 2003; Weinstein et al., 1991) cite cortical generators such as the frontal eye fields or the supplementary eye fields (Bruce & Goldberg, 1985; Funahashi et al., 1991; Goldberg & Bruce, 1990; Mort et al., 2003; Schall, 1991) or subcortical generators (Tsutsui et al., 1987). Of note, it was reported (Balaban & Weinstein, 1985) that the SP is largely absent for spontaneous saccades, which appears to weigh against oculomyographic generators. Additionally, a conference report described several cases of neurological disorders with abnormal SPs (Weinstein & Balaban, 1984).

Regardless of its source, this artifact has proven to be of high concern. Since this artifact is time-locked to saccade initiation and saccades are often correlated with cognitive activity (Engbert & Kliegl, 2003; Kliegl et al., 2006) and psychiatric diagnosis (Gooding & Basso, 2008), any ERP experiment can be affected; even intracranial ERP studies can be affected (Kovach et al., 2011). The amplitude is large enough to survive the averaging process and its positive pole strongly resembles the P300. Furthermore, in the frequency-domain, fast-fourier analysis of this spike artifact results in spurious heightened power in the gamma range (Yuval-Greenberg et al., 2008); a large body of literature on gamma band effects has been thrown into turmoil over this issue (Fries et al., 2008; Reva & Aftanas, 2004; Schwartzman & Kranczioch, 2011; Trujillo et al., 2005; Yuval-Greenberg et al., 2008).

Although some recommend ICA for correction of the saccadic spike potential (Keren et al., 2010; Plöchl et al., 2012), even these authors acknowledge that ICA tends to be unable to isolate it. Unlike the other artifacts, the time course of the saccadic spike potential is short and relatively invariant. Others reported having solved the problem using some form of ICA (Craddock et al., 2016; Dimigen, 2020), but the dimensionality limitations imposed by the number of electrodes in the montage remains a concern. Here we instead follow the lead of a template-based approach (Nottage, 2010) that identified potential SPs using a horizontal electrooculographic or HEOG channel derivation that highlighted spikes with the expected timecourse, confirmed against an averaged spike topography template (Semlitsch et al., 1986), and then removed it from the EEG channels using one of three regression methods that estimated the size of the SP and how it propagated to the EEG channels.

In the MAAC procedure, a similar template procedure is implemented with some improvements. First of all, with the understanding that the SP is likely an unwanted ERP component, not an ocular artifact, the procedure relied on an *a priori* canonical scalp topography

spatial filter (based on the observation that its topography seems quite similar across participants) rather than an EOG channel derivation. Second, the finding that the SP is biphasic was used to further improve detection accuracy. Third, the spatial filter was used directly to determine the contribution to each EEG channel rather than relying on a regression procedure.

One potential complication for this approach is reports that the SP scalp topography appears to shift depending on gaze direction (Keren et al., 2010; Plöchl et al., 2012; Thickbroom & Mastaglia, 1986), but it is necessary to rule out influences from the accompanying CRD effects (Riemslag et al., 1988), which can be difficult. If the SP has a cortical source, it is also possible that this topography shift is due to the asymmetrical control of the contralateral side of space when gaze shifts across the midline (Parks & Corballis, 2008). Regardless, without clear information about saccade direction, it seems best to use a single canonical template since the reported changes in scalp topography appear subtle.

1.5 Movement Artifact

The fourth and final type of artifact correction has not been previously systematically addressed, to this author's knowledge. Head movements can produce high amplitude artifacts in the EEG recordings when they jostle the electrodes, due to the physical disruption of the conducting path between the electrode and the scalp surface. This kind of artifact is especially problematic for existing correction methods because of its extreme non-stationarity, in that both the spatial and temporal characteristics will differ in every instance depending on the nature of the movement and the electrodes affected.

The MAAC addresses this type of artifact by again selecting a procedure that best matches the characteristics of the artifact. Regression is not an option due to the absence of an appropriate predictor variable. ICA is not an option because it requires a substantial number of

observations and this artifact lacks stationarity. Even if sufficient observations can be found to characterize the artifact, there will likely be insufficient dimensionality to characterize all the different instances of movement artifact and yet still characterize the EEG itself.

One approach that can work even with these constraints is PCA with a Promax rotation. Unlike ICA, PCA can operate even with a low number of observations if the variables are highly correlated. As will be demonstrated, a temporal PCA (wherein the time points are the variables and the channels are the observations) is sufficient to characterize a movement artifact in even a single one-second epoch, based on the shared time course of the artifact across channels, as long as it does affect multiple channels. The MAAC procedure is to apply temporal PCA to each epoch in turn, using a Promax rotation that allows for correlations between factors. While it is less effective than more targeted methods, it can also mitigate instances of other artifact types (e.g., blinks) that slip past the prior MAAC stages.

As it currently stands (EP Toolkit 2.91), the full functionality of the EP Toolkit's MAAC is: 1) correct fMRI artifact (Niazy et al., 2005), 2) detect global bad channels, 3) remove mains noise using the PREP (not an acronym) pipeline (Bigdely-Shamlo et al., 2015), 4) saccadic spike potential correction, 5) CRD artifact correction, 6) blink artifact correction, 7) movement artifact correction, 8) remove high-frequency electromyographic or EMG noise (De Vos et al., 2010), 9) mitigate unwanted alpha activity, 10) trial-wise bad channel detection, 11) bad channel correction, and 12) bad trial exclusion. Only most important and novel four steps (4, 5, 6, and 7) will be discussed in depth.

The following steps are conducted by default as part of the MAAC procedure. First it temporarily excludes outlier samples (defined as more than +/-1000 μV from the datasetwise median of that channel). Then it identifies globally bad channels (e.g., defective electrode,

loose contact with scalp, etc.) to be excluded whose best absolute correlation with neighboring channels fell below .4 (across all the timepoints, irrespective of bad trials). In order to detect channels that went bad partway through the session, it divides the session into five sections and tests for bad channels in each. If a channel is bad in at least one such section, it is considered to be globally bad. Furthermore, if a channel has more than 20% timepoints over +/-500 μV from the median in a section, it is also marked bad. Once global bad channels are identified, then any time points that exceed the outlier threshold in at least one of the remaining globally good channels (using a Cz reference) are then marked as bad by replacing them with an NaN value; this is applied to all the channels so that channels far from the recording reference are not disadvantaged.

If the session has more than ten percent bad channels then it is considered a bad participant and it is not further processed. Additionally, flat channels are identified as being bad channels (unless it is identified as being the reference channel). Additionally, channels that correlate perfectly with a reference channel are marked bad (this happens when a file with a flat bad channel is rereferenced).

For the full MAAC (Figure 2), first mains noise is corrected, then a preliminary scan is run to identify blink periods. This scan consists of running the blink correction procedure purely to identify the blink period time points. This scan is further refined by first running a preliminary saccadic spike potential correction to minimize their effect on this preliminary blink scan. After the blink time points are identified, then the actual artifact correction process takes place, first correcting saccadic spike potentials, then the saccadic CRD artifact. After these are corrected, then the true blink correction take place. This is then followed by the movement correction, the EMG artifact correction, and finally the bad data correction.

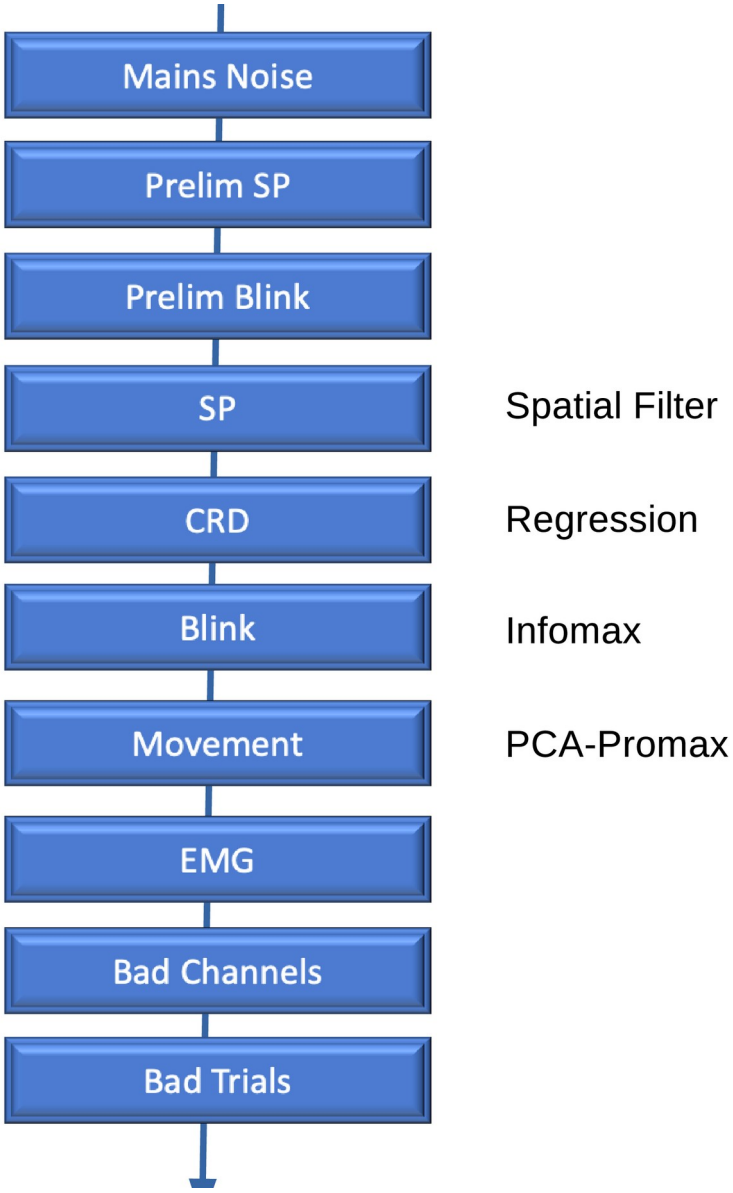

462 Figure 2 - MAAC Flowchart. The order of operations in the MAAC procedure. The algorithms
463 used in the four steps at the focus of this report are also shown.

3.5 Blink Artifact Correction

The MAAC blink auto-template step first identifies epochs (trials in segmented data or one-second periods in unsegmented data) that contain a divergence between the upper and lower vertical electrooculographic or VEOG channels that exceed 150 μV and have a rapid slope onset and offset before and after the peak sample of this divergence. Although simple amplitude thresholds can be problematic (Klein & Skrandies, 2013), the goal here is only to obtain a preliminary sample of high-quality blinks. Alternatively, the EP Toolkit provides a canonical file blink template.

The blink templates are then used to identify blink factors from an ICA based on the correlation of their topographies, as noted in an early description of the MAAC (Frank & Frishkoff, 2007), using the default threshold of .9. These blink factors are then backprojected and deleted from the data.

For the Infomax rotation, the data were first desphered (decorrelated) by performing an initial singular value decomposition retaining the full set of factors, with a subspace reduction via PCA to the rank of the data to minimize overlearning (Särelä & Vigário, 2003). The Infomax rotation (Comon, 1994) is implemented using the runica.m function in EEGLAB (Delorme & Makeig, 2004), with the pseudo-random number generator reinitialized with a "rng(0,'twister')" call prior to each use of Infomax to ensure replicability.

3.6 Corneo-Retinal Dipole Artifact Correction

It is assumed that the combination of a horizontal and a vertical template is sufficient to model the full range of ocular displacements. For an autotemplate, the difference between the

HEOG channels and between the VEOG channels are computed as the initial estimate of the timecourse of the horizontal and vertical components of the CRD. First the horizontal component is subtracted and then the vertical component. This does mean that, to the extent the two are correlated, some portion of the vertical component might end up being attributed to the horizontal component. Alternatively, the EP Toolkit provides a canonical CRD file template that was generated by using an eye-tracker to identify relatively pure horizontal and vertical saccades and using this information to generate horizontal and vertical CRD file templates.

These timecourses are then used as weighting factors while taking a mean scalp topography across the time points, resulting in templates for the horizontal and the vertical components of the CRD artifact. The sign of the weighting factor also takes care of opposite polarity CRD movements so they don't cancel out. In order to keep the algorithm robust against movement artifacts, only the smallest one-eighth of these estimated horizontal movements are used for this procedure; also, the blink periods identified in the preliminary scan are excluded. Finally, this template is used to generate an improved estimate of the CRD movement time course via regression, using the initial rough estimate as the predictor. It is assumed that the saccadic CRD artifact remains present during blinks since it is a consequence of the charged eyeball position, so the blink periods identified in the preliminary scan are also corrected, linearly interpolating from the voltage values just preceding and succeeding them.

This procedure is in some sense the inverse of the Gratton EMCP. Whereas the Gratton EMCP takes the difference between the EOG channels as being the artifact timecourse (removing all of it) and then projecting a best estimate scalp topography from it, this procedure generates an artifact scalp topography and then uses it to project a best estimate timecourse.

3.7 Saccadic Spike Potential Artifact Correction

The next step is to correct SP artifacts. First a preliminary SP detection run is conducted to identify possible SPs. These are then excluded from an initial blink detection procedure (see following description) to identify putative blink time points. Once the putative blink time points are identified, the actual SP correction procedure is conducted using a spatial-filter algorithm. In this step of the MAAC, as for all of them, a guiding principle is to make the algorithms independent of the reference chosen and baseline differences in the waveforms. First, a scan is made for blinks to exclude those time points from the process. The data are then rereferenced to Cz so the process is not affected by variations in referencing. Then the data are transformed into an approximate derivative wherein each point D_t is equal to X_{t+1}- X_t This transformation makes the data independent of the original baselines and highlights sudden voltage changes that are more likely to be due to an SP. Next, a customized SP template is constructed by detecting time points in D where all four VEOG channels spike over a negative threshold that then resolves eight ms later. If all the channels of the putative SP is less than 100 μV (to further exclude artifacts) and the VEOG channels are all more negative than the rest of the channels (not including HEOG channels) then the putative SP is included in the averaged template (Semlitsch et al., 1986). The template is rescaled so that the absolute difference between Cz and the mean of the lower VEOG channels is equal to one. The autotemplate procedure generates two templates (leftward and rightward) whereas the manual template procedure relies on just a single template as it is not clear how one might determine which one to use on the basis of the EEG alone; while such a combined template will therefore be a minor misfit for both directions, it should account for the great majority of the SP artifacts.

This template is then used to generate an amplitude timecourse A by calculating the sum of the channels at each time point of D (excluding the HEOG channels as they are too variable) weighted by the template values. This timecourse A is then used to rescan D for saccadic spike potentials, defined as time points where A exceeds a critical threshold and also exceeds twice the threshold with the opposite polarity either four or eight ms later (the voltages during the offset of the SP are more variable, so a more conservative threshold is needed). If it is confirmed that the upper VEOG channels has a higher mean voltage during the spike than before or after (with a correction factor for the CRD artifact, to be discussed) and also that the putative SP is at least 100 ms after the last identified SP, then it is subtracted based on the amplitude estimated using a least squares fit (Nottage, 2010).

Using an innovative approach, movement artifacts are then removed. A temporal PCA (using the Promax rotation) is conducted. These factors are back-projected and if one had an amplitude (negative to positive peak value) that exceeded 200 μV, it is then deleted from the data.

Using a newly developed method (De Vos et al., 2010) based on blind source separation canonical correlation analysis, the toolkit uses code kindly made available by the developers to remove electromyographic activity and other high-frequency noise. An evaluation of this procedure is outside the scope of the present report and will be addressed elsewhere.

Bad channels are then detected on a trialwise basis. They are defined as having a difference of more than 100 μV from the minimum and the maximum values in that trial. They are also declared bad when the maximum divergence from all the other channels is computed and even the least different is 30+ μV (so all the other channels were quite different). Flat

channels are also marked as being bad, unless they are identified as being a reference channel AND the channel is flat over the entire dataset. If more than 10% of the channels (including globally bad channels) are marked as bad then the entire trial is marked bad. If a channel is marked as bad on more than 20% of the good trials, then it is marked as globally bad. Channels that are marked bad are replaced via biharmonic splines and bad trials are zeroed out.

4.0 MAAC Preprocessing Example

This final section provides an example of how the MAAC is implemented in the EP Toolkit to provide readers a better sense of what it would be like to use this method in their workflow. It also provides some general guidance of how to interpret the output and how to adjust the settings when needed, based on the preceding review of artifact types and correction methods. For a full explanation of how to utilize the EP Toolkit, including the MAAC, interested readers are directed to the comprehensive tutorial that is provided as part of the EP Toolkit in its Documentation directory. The EP Toolkit can be downloaded for free from: https://sourceforge.net/projects/erppcatoolkit/

For this example, we will use one session a dataset wherein the participant read a full paragraph with no constraints, resulting in many saccades and blinks. For illustrating the effect on the final event-related potential, for simplicity's sake we'll just examine the fixation-related potential.

4.1 MAAC Settings

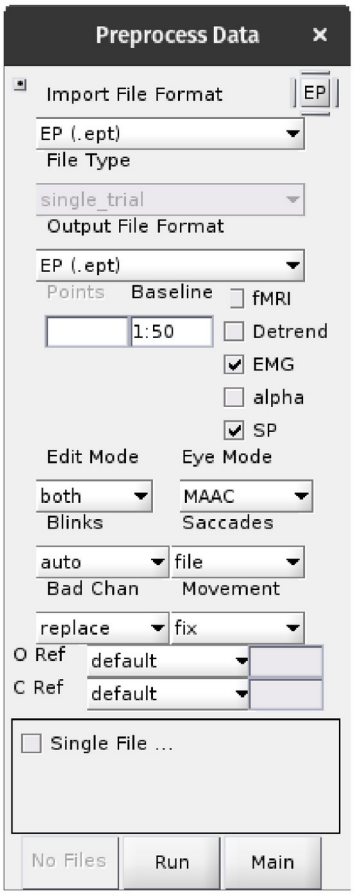

571 Figure 3 - MAAC Interface. The EP Toolkit graphical user interface for applying the MAAC to
572 datasets.

In Figure 3, we can see the Preprocessing pane settings used for this example. See the EP Toolkit documentation for more information about the settings. Once everything is ready, one then clicks on "Run" to select a batch of files for preprocessing.

4.2 MAAC Quality Control Output

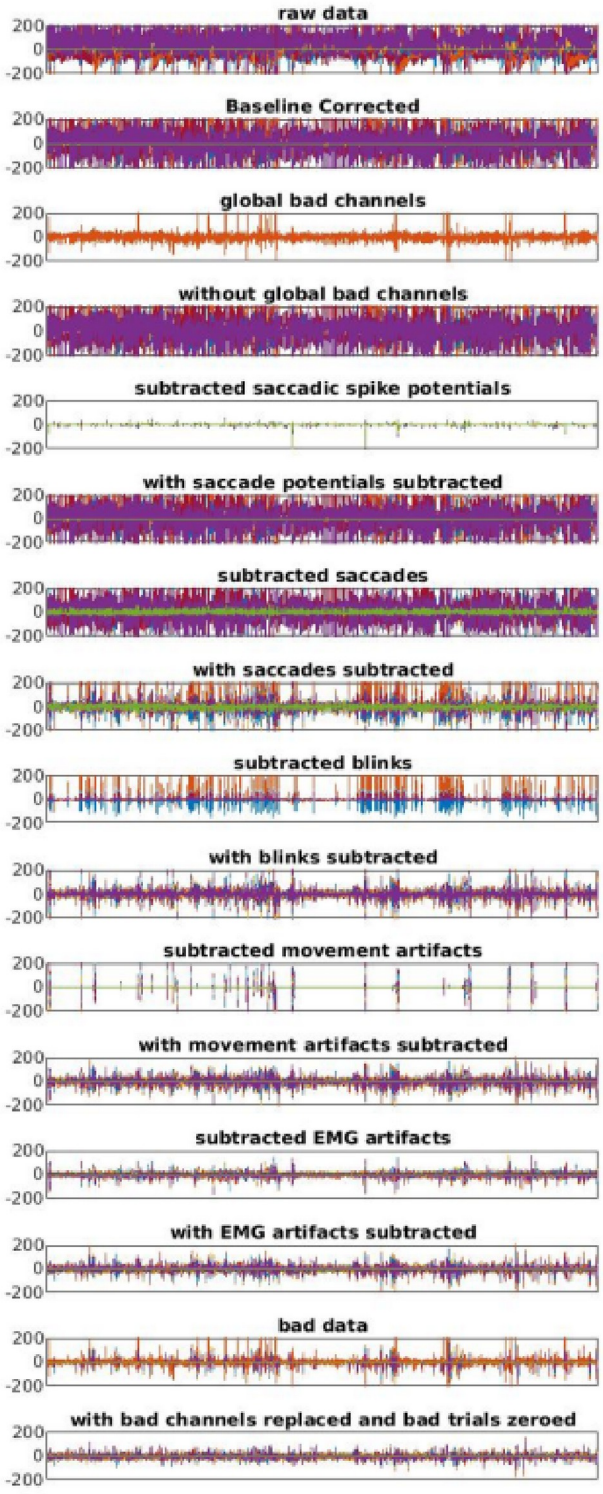
raw data
200
0
-200
Baseline Corrected
200
0
-200
global bad channels
200
0
-200
without global bad channels
200
0
-200
subtracted saccadic spike potentials
200
0
-200
with saccade potentials subtracted
200
0
-200
subtracted saccades
200
0
-200
with saccades subtracted
200
0
-200
subtracted blinks
200
0
-200
with blinks subtracted
200
0
-200
subtracted movement artifacts
200
0
-200
with movement artifacts subtracted
200
0
-200
subtracted EMG artifacts
200
0
-200
with EMG artifacts subtracted
200
0
-200
bad data
200
0
-200
with bad channels replaced and bad trials zeroed
200
0
-200

Figure 4 - MAAC Summary Output Figure. The primary quality control figure, showing each step of the preprocessing procedure.

In Figure 4, the summary quality control figure for the MAAC output of this example file is provided. Each line represents one step in the procedure, in the form of a butterfly plot, in which the entire file is displayed end-to-end, with each colored line representing one of the channels superimposed on each other. The scale of each plot is -/+200 μV. This plot provides a general sense of the noise levels and highlights anomalous bursts of activity that may represent artifacts:

1) *raw data* shows the initial uncorrected data. As can be seen, it is quite noisy, given that true EEG activity should not exceed about 20 μV.

2) *Baseline Corrected* shows the same data but now the data have been baseline corrected, centering all of the channels. Since this dataset was already segmented, each epoch was free to be individually adjusted, thus resulting in the equivalent of a lossless high-pass filter. While not an option for unsegmented data, one can instead detrend the data, which still provides some benefit.

3) *global bad channels* shows the channels identified as being globally bad channels (as opposed to trialwise bad channels).

4) *without global bad channels* shows the data with the global bad channels excluded. They will be excluded from this point onwards.

5) *subtracted saccadic spike potentials* shows the activity identified as being due to saccadic spike potentials.

6) *with saccade potentials subtracted* shows the data with the saccadic spike potentials removed. They will be excluded from this point onwards. Although the amplitude of the artifacts

are small, they can be problematic as they can be event-locked and their scalp topography greatly resembles that of the P300.

7) *subtracted saccades* shows the activity identified as being due to saccadic CRD artifacts. Note that this activity can be quite high amplitude, hence the need to remove it, especially if frontal electrodes are of interest.

8) *with saccades subtracted* shows the data with the saccadic CRD artifacts removed. They will be excluded from this point onwards.

9) *subtracted blinks* shows the activity identified as being due to blink artifacts. They tend to present themselves as high amplitude spikes with a relatively stable ratio between the negative channels and the positive channels. Also, the channels involved (as depicted by the colors) should be stable throughout.

10) *with blinks subtracted* shows the data with the blink artifacts removed. They will be excluded from this point onwards. A successful blink correction will have removed the blink-like artifacts whereas a failure will leave them still present.

11) *subtracted movement artifacts* shows the activity identified as being due to movement artifacts. Movement artifacts by their nature are quite idiosyncratic, depending on the movement involved. One therefore expects them to be all different.

12) *with movement artifacts subtracted* shows the data with the movement artifacts removed. They will be excluded from this point onwards.

13) *subtracted EMG artifacts* shows the activity identified as being EMG artifacts.

14) *with EMG artifacts* subtracted shows the data with the EMG artifacts removed. They will be excluded from this point onwards.

15) *bad data* shows the activity identified as being bad data. This includes both global bad channels as well as trialwise bad channels and bad epochs. The trialwise bad data identification is based on the data as corrected by the preceding steps.

16) *with bad channels replaced and bad trials zeroed* shows the data with the bad channels replaced via interpolation (if that was the chosen option) and bad trials simply zeroed out. The latter will be ignored during subsequent steps in the analysis stream.

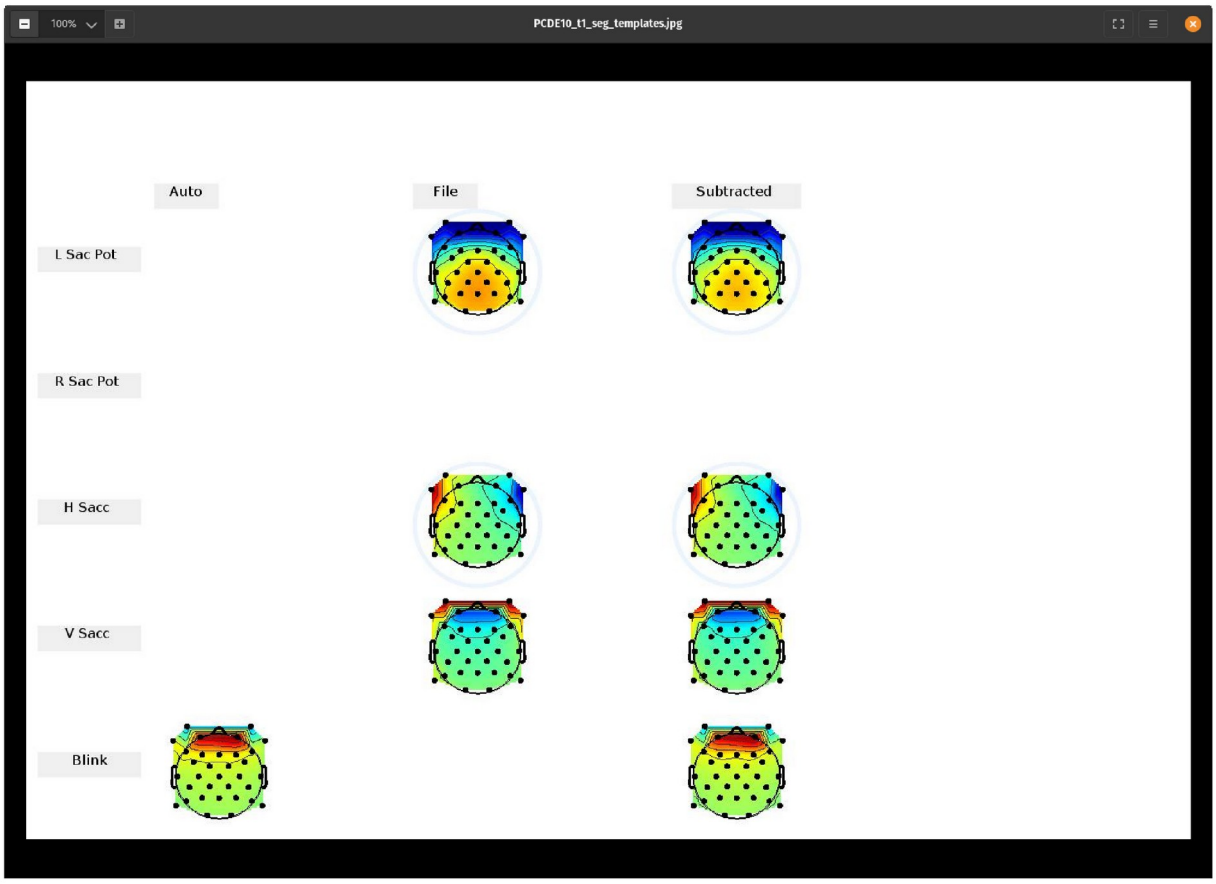

628 Figure 5 - MAAC Template Output Figure. An additional quality control figure provided by the
629 EP Toolkit, displaying the scalp topographies of the templates.

In Figure 5, the MAAC templates output figure is presented. This figure provides the scalp topographies of the templates used during the artifact correction process (these templates are the averaged artifacts from real data). This output file should be examined for each session to verify that it was done properly. This example demonstrates what a successful output looks like. On the first line is the topography of the high-quality canonical saccadic spike potential, as obtained from the file template accompanying the EP Toolkit. By default, the file template is used for all such corrections (there is also an automatic option, but informal testing suggests it is less effective). Although the figure allows for separate left and right SP templates, since the topography difference is small and it would require additional eye-tracker information to know which to use, here only one template is used. In all cases, the final column shows the grand average scalp topography actually subtracted from the dataset, which for the MAAC will have the same topography as the templates.

The third row is for horizontal saccadic CRD artifacts. The first column is blank because the "file" option was chosen. The second column shows the canonical horizontal CRD scalp topography provided by the EP Toolkit. The template is arbitrarily scaled to depict a rightward horizontal CRD. The fourth row is for the vertical saccadic CRD artifacts. The second column shows the canonical vertical CRD scalp topography provided by the EP Toolkit. The template is arbitrarily scaled to depict an upward vertical CRD. The fifth row is for the blink artifacts. Since the "auto" option was chosen, there is only a template in the first column. It illustrates the typical blink topography with the inversion above and below the eye sockets, with the upper ones being positive. It is quite similar to that of the vertical CRD artifact, making them hard to differentiate.

Blink correction in particular requires visual confirmation. Because blink artifacts are quite stereotyped, this step will tend to either successfully identify the vast majority of the blinks or it will entirely fail. Sometimes blink correction will fail to detect blinks because there are none to find. Because of the similarity between the topography of vertical saccadic CRD artifacts and blink artifacts, sometimes the former step will mistakenly correct blink artifacts as well. This would be an indication that neither was being fully corrected and would need to be fixed. If this happens, it is due to the preliminary blink detection step not working, so that is what would need fixing. If blinks were missed by both steps, then they will be corrected during the movement correction step, but the accuracy of the correction is expected to be lower than if they were properly corrected during the blink correction step.

There are two major ways of fixing blink correction problems. The first is to manually construct a blink template for the problematic session, which the EP Toolkit facilitates with a full graphical user interface. Alternatively, if the text log output (which the EP Toolkit also provides) indicates that the best candidate for a blink factor only just missed the threshold (default of .90), then one could reduce the threshold and rerun. Note that the lower the threshold, the more likely it is that false positives could happen, with non-blink factors also being corrected. This threshold setting can be accessed by clicking on the small button in the upper left corner of the Preprocessing pane, which brings up the associated preferences pane. Again, this section is just meant to provide a sense of the user experience. For a full explanation of how to use the MAAC, see the Tutorial that accompanies the EP Toolkit.

5.0 Conclusion

In conclusion, this report has made the argument that efforts to identify a "best" artifact correction method (e.g., ICA) is ill-posed. Instead, by describing in detail the four major sources

of artifact and their properties, it can be seen that each is best addressed with a different method. The MAAC is the first to take such a principled approach to artifact correction and to make it easy to use, as demonstrated in the final section. Two accompanying reports provide empirical support for the argument that a single method such as ICA cannot be the best way to address such diverse artifacts (Dien et al., 2024) and provide an empirical comparison of its performance against competing artifact correction software (Dien & O'Hare, 2024).

Declaration of Generative AI and AI-assisted technologies in the writing process

The author did not use generative AI technologies for preparation of this work.

683 **References**

Anderer, P., Roberts, S., Schlögl, A., Gruber, G., Klösch, G., Herrmann, W., Rappelsberger, P., Filz, O., Barbanoj, M. J., Dorffner, G., & Saletu, B. (1999). Artifact Processing in Computerized Analysis of Sleep EEG – A Review. *Neuropsychobiology*, *40*(3), 150–157. https://doi.org/10.1159/000026613

Arden, G. B., & Constable, P. A. (2006). The electro-oculogram. *Progress in Retinal and Eye Research*, *25*(2), 207–248. https://doi.org/10.1016/j.preteyeres.2005.11.001

Balaban, C. D., & Weinstein, J. M. (1985). The human pre-saccadic spike potential: Influences of a visual target, saccade direction, electrode laterality and instructions to perform saccades. *Brain Research*, *347*(1), 49–57. https://doi.org/10.1016/0006-8993(85)90888-1

Bell, A. J., & Sejnowski, T. J. (1995). An information-maximisation approach to blind separation and blind deconvolution. *Neural Computation*, *7*(6), 1129–1159. https://doi.org/10.1162/neco.1995.7.6.1129

Berg, P. (1986). The Residual After Correcting Event-Related Potentials for Blink Artifacts. *Psychophysiology*, *23*(3), 354–364. https://doi.org/10.1111/j.1469-8986.1986.tb00646.x

Berg, P., & Scherg, M. (1991). Dipole models of eye movements and blinks. *Electroencephalography and Clinical Neurophysiology*, *79*(1), 36–44. https://doi.org/10.1016/0013-4694(91)90154-V

Berg, P., & Scherg, M. (1994). A multiple source approach to the correction of eye artifacts. *Electroencephalography and Clinical Neurophysiology*, *90*(3), 229–241. https://doi.org/10.1016/0013-4694(94)90094-9

Bigdely-Shamlo, N., Mullen, T., Kothe, C., Su, K.-M., & Robbins, K. A. (2015). The PREP pipeline: Standardized preprocessing for large-scale EEG analysis. *Frontiers in Neuroinformatics*, *9*. https://doi.org/10.3389/fninf.2015.00016

Blinn, K. A. (1955). Focal anterior temporal spikes from external rectus muscle. *Electroencephalography and Clinical Neurophysiology*, *7*(2), 299–302. https://doi.org/10.1016/0013-4694(55)90043-2

Boylan, C., & Doig, H. R. (1988). Presaccadic spike potential to horizontal eye movements. *Electroencephalography and Clinical Neurophysiology*, *70*(6), 559–562. https://doi.org/10.1016/0013-4694(88)90153-8

Brickett, P. A., Weinberg, H., & Davis, C. M. (1984). Cerebral potentials preceding visually triggered saccades. *Annals of the New York Academy of Sciences*, *425*, 429–433. https://doi.org/10.1111/j.1749-6632.1984.tb23563.x

Bruce, C. J., & Goldberg, M. E. (1985). Primate frontal eye fields. I. Single neurons discharging before saccades. *Journal of Neurophysiology*, *53*(3), 603–635. https://doi.org/10.1152/jn.1985.53.3.603

Brunia, C. H., Möcks, J., Van den Berg-Lenssen, M. M., Coelho, M., & et al. (1989). Correcting ocular artifacts in the EEG: A comparison of several models. *Journal of Psychophysiology*, *3*(1), 1–50.

Brunyé, T. T., & Gardony, A. L. (2017). Eye tracking measures of uncertainty during perceptual decision making. *International Journal of Psychophysiology*, *120*, 60–68. https://doi.org/10.1016/j.ijpsycho.2017.07.008

Carl, C., Açık, A., König, P., Engel, A. K., & Hipp, J. F. (2012). The saccadic spike artifact in MEG. *Neuroimage*, *59*(2), 1657–1667. https://doi.org/10.1016/j.neuroimage.2011.09.020

Castellanos, N. P., & Makarov, V. A. (2006). Recovering EEG brain signals: Artifact suppression with wavelet enhanced independent component analysis. *Journal of Neuroscience Methods*, *158*(2), 300–312. https://doi.org/10.1016/j.jneumeth.2006.05.033

Chapman, R. M., & McCrary, J. W. (1995). EP component identification and measurement by principal components analysis. *Brain and Cognition*, *27*(3), 288–310. https://doi.org/10.1006/brcg.1995.1024

Coles, M. G. H., & Gratton, G. (1989). Generalization and evaluation of eye-movement correction procedures. *Journal of Psychophysiology*, *3*, 14–16.

Comon, P. (1994). Independent component analysis, A new concept? *Signal Processing*, *36*(3), 287–314. https://doi.org/10.1016/0165-1684(94)90029-9

Corby, J. C., & Kopell, B. S. (1972). Differential Contributions of Blinks and Vertical Eye Movements as Artifacts in EEG Recording. *Psychophysiology*, *9*(6), 640–644. https://doi.org/10.1111/j.1469-8986.1972.tb00776.x

Craddock, M., Martinovic, J., & Müller, M. M. (2016). Accounting for microsaccadic artifacts in the EEG using independent component analysis and beamforming. *Psychophysiology*, *53*(4), 553–565. https://doi.org/10.1111/psyp.12593

Croft, R. J., & Barry, R. J. (2000). Removal of ocular artifact from the EEG: A review. *Neurophysiologie Clinique/Clinical Neurophysiology*, *30*(1), 5–19. https://doi.org/10.1016/S0987-7053(00)00055-1

Csibra, G., Johnson, M. H., & Tucker, L. A. (1997). Attention and oculomotor control: A high-density ERP study of the gap effect. *Neuropsychologia*, *35*(6), 855–865. https://doi.org/10.1016/S0028-3932(97)00016-X

De Vos, M., Vos, de M., Riès, S., Vanderperren, K., Vanrumste, B., Alario, F. X., Van Huffel, S., Huffel, V. S., & Burle, B. (2010). Removal of muscle artifacts from EEG recordings of

spoken language production. *Neuroinformatics*, *8*(2), 135–150. https://doi.org/10.1007/s12021-010-9071-0

Delorme, A., & Makeig, S. (2004). EEGLAB: An open source toolbox for analysis of single-trial EEG dynamics including independent component analysis. *Journal of Neuroscience Methods*, *134*(1), 9–21. https://doi.org/10.1016/j.jneumeth.2003.10.009

Delorme, A., Sejnowski, T., & Makeig, S. (2007). Enhanced detection of artifacts in EEG data using higher-order statistics and independent component analysis. *NeuroImage*, *34*(4), 1443–1449. https://doi.org/10.1016/j.neuroimage.2006.11.004

Dien, J. (1998). Addressing misallocation of variance in principal components analysis of event-related potentials. *Brain Topography*, *11*(1), 43–55. https://doi.org/10.1023/A:1022218503558

Dien, J. (2010a). Evaluating Two-Step PCA Of ERP Data With Geomin, Infomax, Oblimin, Promax, And Varimax Rotations. *Psychophysiology*, *47*(1), 170–183. https://doi.org/10.1111/j.1469-8986.2009.00885.x

Dien, J. (2010b). The ERP PCA Toolkit: An Open Source Program For Advanced Statistical Analysis of Event Related Potential Data. *Journal of Neuroscience Methods*, *187*(1), 138–145. https://doi.org/10.1016/j.jneumeth.2009.12.009

Dien, J. (2012). Applying Principal Components Analysis to Event Related Potentials: A Tutorial. *Developmental Neuropsychology*, *37*(6), 497–517. https://doi.org/10.1080/87565641.2012.697503

Dien, J., Beal, D. J., & Berg, P. (2005). Optimizing principal components analysis of event-related potential analysis: Matrix type, factor loading weighting, extraction, and rotations. *Clinical Neurophysiology*, *116*(8), 1808–1825. https://doi.org/10.1016/j.clinph.2004.11.025

Dien, J., & Frishkoff, G. A. (2005). Principal components analysis of event-related potential datasets. In T. Handy (Ed.), *Event-Related Potentials: A Methods Handbook* (pp. 189–208). MIT Press.

Dien, J., Gwizdka, J., Kogut, P., Lo, L.-C., Oh, H., & Jaquess, K. J. (2024). *Multi-Algorithm Artifact Correction (MAAC) Procedure Part Two: Is Independent Components Analysis the Best Choice for Blink, Corneo-Retinal Dipole, Saccadic Spike Potential, and Movement Artifact Correction?* [Manuscript submitted for publication].

Dien, J., Khoe, W., & Mangun, G. R. (2007). Evaluation of PCA and ICA of simulated ERPs: Promax versus Infomax rotations. *Human Brain Mapping*, *28*(8), 742–763. https://doi.org/10.1002/hbm.20304

Dien, J., & O'Hare, A. (2024). *Multi-Algorithm Artifact Correction (MAAC) Procedure Part Three: Choosing the Wrong Preprocessing Program Can Destroy Your Experiment* [Manuscript submitted for publication].

Dien, J., Spencer, K. M., & Donchin, E. (2003). Localization of the event-related potential novelty response as defined by principal components analysis. *Cognitive Brain Research*, *17*(3), 637–650. https://doi.org/10.1016/S0926-6410(03)00188-5

Dimigen, O. (2020). Optimizing the ICA-based removal of ocular EEG artifacts from free viewing experiments. *NeuroImage*, *207*, 116117. https://doi.org/10.1016/j.neuroimage.2019.116117

Donchin, E. (1966). A multivariate approach to the analysis of average evoked potentials. *IEEE Transactions on Bio-Medical Engineering*, *BME-13*, 131–139. https://doi.org/10.1109/TBME.1966.4502423

Elbert, T., Lutzenberger, W., Rockstroh, B., & Birbaumer, N. (1985). Removal of ocular artifacts from the EEG — A biophysical approach to the EOG. *Electroencephalography and*

Clinical Neurophysiology, *60*(5), 455–463. https://doi.org/10.1016/0013-4694(85)91020-X

Engbert, R., & Kliegl, R. (2003). Microsaccades uncover the orientation of covert attention. *Vision Res*, *43*(9), 1035–1045. https://doi.org/10.1016/S0042-6989(03)00084-1

Fatourechi, M., Bashashati, A., Ward, R. K., & Birch, G. E. (2007). EMG and EOG artifacts in brain computer interface systems: A survey. *Clinical Neurophysiology*, *118*(3), 480–494. https://doi.org/10.1016/j.clinph.2006.10.019

Fischer, H. (2010). *A history of the central limit theorem: From classical to modern probability theory*. Springer Science & Business Media.

Fog, C. V. M. (1964). The Dependence of Corneo-Retinal Potential upon Illumination. *Acta Oto-Laryngologica*, *57*(sup188), 414–420. https://doi.org/10.3109/00016486409134596

Fogarty, C., & Stern, J. A. (1989). Eye movements and blinks: Their relationship to higher cognitive processes. *International Journal of Psychophysiology*, *8*(1), 35–42. https://doi.org/10.1016/0167-8760(89)90017-2

Frank, R. M., & Frishkoff, G. A. (2007). Automated protocol for evaluation of electromagnetic component separation (APECS): Application of a framework for evaluating statistical methods of blink extraction from multichannel EEG. *Clinical Neurophysiology*, *118*(1), 80–97. https://doi.org/10.1016/j.clinph.2006.07.317

Fries, P., Scheeringa, R., & Oostenveld, R. (2008). Finding gamma. *Neuron*, *58*(3), 303–305. https://doi.org/10.1016/j.neuron.2008.04.020

Funahashi, S., Bruce, C. J., & Goldman-Rakic, P. S. (1991). Neuronal activity related to saccadic eye movements in the monkey's dorsolateral prefrontal cortex. *Journal of Neurophysiology*, *65*(6), 1464–1483. https://doi.org/10.1152/jn.1991.65.6.1464

Gao, J. F., Yang, Y., Lin, P., Wang, P., & Zheng, C. X. (2010). Automatic Removal of Eye-Movement and Blink Artifacts from EEG Signals. *Brain Topography*, *23*(1), 105–114. https://doi.org/10.1007/s10548-009-0131-4

Ghaderi, F., Kim, S. K., & Kirchner, E. A. (2014). Effects of eye artifact removal methods on single trial P300 detection, a comparative study. *Journal of Neuroscience Methods*, *221*, 41–47. https://doi.org/10.1016/j.jneumeth.2013.08.025

Goldberg, M. E., & Bruce, C. J. (1990). Primate frontal eye fields. III. Maintenance of a spatially accurate saccade signal. *Journal of Neurophysiology*, *64*(2), 489–508. https://doi.org/10.1152/jn.1990.64.2.489

Gooding, D. C., & Basso, M. A. (2008). The tell-tale tasks: A review of saccadic research in psychiatric patient populations. *Brain and Cognition*, *68*(3), 371–390. https://doi.org/10.1016/j.bandc.2008.08.024

Gorsuch, R. L. (1983). *Factor analysis* (2nd ed.). Lawrence Erlbaum Associates.

Gratton, G., Coles, M. G. H., & Donchin, E. (1983). A new method for off-line removal of ocular artifact. *Electroencephalography and Clinical Neurophysiology*, *55*(3), 468–484. https://doi.org/10.1016/0013-4694(83)90135-9

Gratton, G., Coles, M. G. H., & Donchin, E. (1989). A procedure for using multi-electrode information in the analysis of components of the event-related potential: Vector filter. *Psychophysiology*, *26*(2), 222–232. https://doi.org/10.1111/j.1469-8986.1989.tb03160.x

Haumann, N. T., Parkkonen, L., Kliuchko, M., Vuust, P., & Brattico, E. (2016). *Comparing the Performance of Popular MEG/EEG Artifact Correction Methods in an Evoked-Response Study*. Computational Intelligence and Neuroscience; Hindawi. https://doi.org/10.1155/2016/7489108

Hendrickson, A. E., & White, P. O. (1964). Promax: A quick method for rotation to oblique simple structure. *The British Journal of Statistical Psychology*, *17*(1), 65–70. https://doi.org/10.1111/j.2044-8317.1964.tb00244.x

Hess, C. W., Muri, R., & Meienberg, O. (1986). Recording of Horizontal Saccadic Eye Movements: Methodological Comparison Between Electro-Oculography and Infrared Reflection Oculography. *Neuro-Ophthalmology*, *6*(3), 189–197. https://doi.org/10.3109/01658108608997351

Hillyard, S. A., & Galambos, R. (1970). Eye movement artifact in the CNV. *Electroencephalography and Clinical Neurophysiology*, *28*(2), 173–182. https://doi.org/10.1016/0013-4694(70)90185-9

Hipp, J. F., & Siegel, M. (2013). Dissociating neuronal gamma-band activity from cranial and ocular muscle activity in EEG. *Frontiers in Human Neuroscience*, *7*. https://doi.org/10.3389/fnhum.2013.00338

Hoffmann, S., & Falkenstein, M. (2008). The Correction of Eye Blink Artefacts in the EEG: A Comparison of Two Prominent Methods. *PLOS ONE*, *3*(8), e3004. https://doi.org/10.1371/journal.pone.0003004

Hyvärinen, A., Karhunen, J., & Oja, E. (2001). *Independent Component Analysis*. John Wiley & Sons.

Ifeachor, E. C., Jervis, B. W., Allen, E. M., Morris, E. L., Wright, D. E., & Hudson, N. R. (1988). Investigation and comparison of some models for removing ocular artefacts from EEG signals. *Medical and Biological Engineering and Computing*, *26*(6), 591–598. https://doi.org/10.1007/BF02447496

Ille, N., Berg, P., & Scherg, M. (2002). Artifact Correction of the Ongoing EEG Using Spatial Filters Based on Artifact and Brain Signal Topographies. *Journal of Clinical Neurophysiology*, *19*(2), 113.

Iwasaki, M., Kellinghaus, C., Alexopoulos, A. V., Burgess, R. C., Kumar, A. N., Han, Y. H., Lüders, H. O., & Leigh, R. J. (2005). Effects of eyelid closure, blinks, and eye movements on the electroencephalogram. *Clinical Neurophysiology*, *116*(4), 878–885. https://doi.org/10.1016/j.clinph.2004.11.001

Jervis, B. W., Ifeachor, E. C., & Allen, E. M. (1988). The removal of ocular artefacts from the electroencephalogram: A review. *Medical and Biological Engineering and Computing*, *26*(1), 2–12. https://doi.org/10.1007/BF02441820

Joyce, C. A., Gorodnitsky, I. F., & Kutas, M. (2004). Automatic removal of eye movement and blink artifacts from EEG data using blind component separation. *Psychophysiology*, *41*(2), 313–325. https://doi.org/10.1111/j.1469-8986.2003.00141.x

Jung, T.-P., Humphries, C., W., L. T., Makeig, S., McKeown, M. J., Iragui, V., & Sejnowski, T. J. (1997). Extended ICA removes artifacts from electroencephalographic recordings. *Advances in Neural Information Processing Systems*, *10*, 894–900.

Jung, T.-P., Makeig, S., Westerfield, M., Townsend, J., Courchesne, E., & Sejnowski, T. J. (2000). Removal of eye activity artifacts from visual event-related potentials in normal and clinical subjects. *Clinical Neurophysiology*, *111*(10), 1745–1758. https://doi.org/10.1016/S1388-2457(00)00386-2

Kaczorowska, M., Plechawska-Wojcik, M., Tokovarov, M., & Dmytruk, R. (2017). Comparison of the ICA and PCA methods in correction of EEG signal artefacts. *2017 10th International Symposium on Advanced Topics in Electrical Engineering (ATEE)*, 262–267. https://doi.org/10.1109/ATEE.2017.7905095

Kaiser, H. F. (1958). The varimax criterion for analytic rotation in factor analysis. *Psychometrika*, *23*(3), 187–200. https://doi.org/10.1007/BF02289233

Keren, A. S., Yuval-Greenberg, S., & Deouell, L. Y. (2010). Saccadic spike potentials in gamma-band EEG: characterization, detection and suppression. *Neuroimage*, *49*(3), 2248–2263. https://doi.org/10.1016/j.neuroimage.2009.10.057

Kierkels, J. J. M., Riani, J., Bergmans, J. W. M., & van Boxtel, G. J. M. (2007). Using an Eye Tracker for Accurate Eye Movement Artifact Correction. *IEEE Transactions on Biomedical Engineering*, *54*(7), 1256–1267. https://doi.org/10.1109/TBME.2006.889179

Kirkove, M., François, C., & Verly, J. (2014). Comparative evaluation of existing and new methods for correcting ocular artifacts in electroencephalographic recordings. *Signal Processing*, *98*, 102–120. https://doi.org/10.1016/j.sigpro.2013.11.015

Klein, A., & Skrandies, W. (2013). A Reliable Statistical Method to Detect Eyeblink-Artefacts from Electroencephalogram Data Only. *Brain Topography*, *26*(4), 558–568. https://doi.org/10.1007/s10548-013-0281-2

Kliegl, R., Nuthmann, A., & Engbert, R. (2006). Tracking the mind during reading: The influence of past, present, and future words on fixation durations. *Journal of Experimental Psychology: General*, *135*(1), 12–35. https://doi.org/10.1037/0096-3445.135.1.12

Kong, W., Zhou, Z., Hu, S., Zhang, J., Babiloni, F., & Dai, G. (2013). Automatic and Direct Identification of Blink Components from Scalp EEG. *Sensors*, *13*(8), Article 8. https://doi.org/10.3390/s130810783

Kovach, C. K., Tsuchiya, N., Kawasaki, H., Oya, H., Howard, M. A., & Adolphs, R. (2011). Manifestation of ocular-muscle EMG contamination in human intracranial recordings. *Neuroimage*, *54*(1), 213–233. https://doi.org/10.1016/j.neuroimage.2010.08.002

Kurtzberg, D., & Vaughan, H. G. (1982). Topographic analysis of human cortical potentials preceding self-initiated and visually triggered saccades. *Brain Research*, *243*(1), 1–9. https://doi.org/10.1016/0006-8993(82)91115-5

Lagerlund, T. D., Sharbrough, F. W., & Busacker, N. E. (1997). Spatial filtering of multichannel electroencephalographic recordings through principal component analysis by singular value decomposition. *Journal of Clinical Neurophysiology*, *14*(1), 73–82.

LeVan, P., Urrestarazu, E., & Gotman, J. (2006). A system for automatic artifact removal in ictal scalp EEG based on independent component analysis and Bayesian classification. *Clinical Neurophysiology*, *117*(4), 912–927. https://doi.org/10.1016/j.clinph.2005.12.013

Lins, O. G., Picton, T. W., Berg, P., & Scherg, M. (1993a). Ocular artifacts in EEG and event-related potentials. I: Scalp topography. *Brain Topography*, *6*(1), 51–63. https://doi.org/10.1007/BF01234127

Lins, O. G., Picton, T. W., Berg, P., & Scherg, M. (1993b). Ocular artifacts in recording EEGs and event-related potentials. II: Source dipoles and source components. *Brain Topography*, *6*(1), 65–78. https://doi.org/10.1007/BF01234128

Makeig, S., Bell, A. J., Jung, T., & Sejnowski, T. J. (1996). Independent component analysis of electroencephalographic data. *Advances in Neural Information Processing Systems*, *8*, 145–151.

Mammone, N., & Morabito, F. C. (2008). Enhanced automatic artifact detection based on independent component analysis and Renyi's entropy. *Neural Networks*, *21*(7), 1029–1040. https://doi.org/10.1016/j.neunet.2007.09.020

Mannan, M. M. N., Jeong, M. Y., & Kamran, M. A. (2016). Hybrid ICA—Regression: Automatic Identification and Removal of Ocular Artifacts from Electroencephalographic Signals. *Frontiers in Human Neuroscience*, *10*. https://doi.org/10.3389/fnhum.2016.00193

Matsuo, F., Peters, J. F., & Reilly, E. L. (1975). Electrical phenomena associated with movements of the eyelid. *Electroencephalography and Clinical Neurophysiology*, *38*(5), 507–511. https://doi.org/10.1016/0013-4694(75)90191-1

Mennes, M., Wouters, H., Vanrumste, B., Lagae, L., & Stiers, P. (2010). Validation of ICA as a tool to remove eye movement artifacts from EEG/ERP. *Psychophysiology*, *47*(6), 1142–1150. https://doi.org/10.1111/j.1469-8986.2010.01015.x

Mort, D. J., Perry, R. J., Mannan, S. K., Hodgson, T. L., Anderson, E., Quest, R., McRobbie, D., McBride, A., Husain, M., & Kennard, C. (2003). Differential cortical activation during voluntary and reflexive saccades in man. *Neuroimage*, *18*(2), 231–246. https://doi.org/10.1016/S1053-8119(02)00028-9

Moster, M. L., & Goldberg, G. (1990). Topography of scalp potentials preceding self-initiated saccades. *Neurology*, *40*(4), 644–648. https://doi.org/10.1212/WNL.40.4.644

Nativ, A., Weinstein, J. M., & Rosas-Ramos, R. (1990). Human presaccadic spike potentials. Of central or peripheral origin. *Investigative Ophthalmology & Visual Science*, *31*(9), 1923–1928.

Niazy, R. K., Beckmann, C. F., Iannetti, G. D., Brady, J. M., & Smith, S. M. (2005). Removal of FMRI environment artifacts from EEG data using optimal basis sets. *Neuroimage*, *28*(3), 720–737. https://doi.org/10.1016/j.neuroimage.2005.06.067

Nottage, J. F. (2010). Uncovering gamma in visual tasks. *Brain Topography*, *23*(1), 58–71. https://doi.org/10.1007/s10548-009-0129-y

Ochoa, C. J., & Polich, J. (2000). P300 and blink instructions. *Clinical Neurophysiology*, *111*(1), 93–98. https://doi.org/10.1016/S1388-2457(99)00209-6

Onton, J., Westerfield, M., Townsend, J., & Makeig, S. (2006). Imaging human EEG dynamics using independent component analysis. *Neuroscience & Biobehavioral Reviews*, *30*(6), 808–822. https://doi.org/10.1016/j.neubiorev.2006.06.007

Overton, D., & Shagass, C. (1969). Distribution of eye movement and eyeblink potentials over the scalp. *Electroencephalography and Clinical Neurophysiology*, *27*(5), 546.

Parks, N. A., & Corballis, P. M. (2008). Electrophysiological correlates of presaccadic remapping in humans. *Psychophysiology*, *45*(5), 776–783. https://doi.org/10.1111/j.1469-8986.2008.00669.x

Peters, J. F. (1967). Surface Electrical Fields Generated by Eye Movements. *American Journal of EEG Technology*, *7*(2), 27–40. https://doi.org/10.1080/00029238.1967.11080683

Picton, T. W., van Roon, P., Armilio, M. L., Berg, P., Ille, N., & Scherg, M. (2000a). Blinks, saccades, extraocular muscles and visual evoked potentials (Reply to Verleger). *Journal of Psychophysiology*, *14*(4), 210–217. https://doi.org/10.1027/0269-8803.14.4.210

Picton, T. W., van Roon, P., Armilio, M. L., Berg, P., Ille, N., & Scherg, M. (2000b). The correction of ocular artifacts: A topographic perspective. *Clinical Neurophysiology*, *111*(1), 53–65. https://doi.org/10.1016/S1388-2457(99)00227-8

Plöchl, M., Ossandon, J. P., & Konig, P. (2012). Combining EEG and eye tracking: Identification, characterization, and correction of eye movement artifacts in electroencephalographic data. *Frontiers in Human Neuroscience*, *6*, 278. https://doi.org/10.3389/fnhum.2012.00278

Reva, N. V., & Aftanas, L. I. (2004). The coincidence between late non-phase-locked gamma synchronization response and saccadic eye movements. *International Journal of Psychophysiology*, *51*(3), 215–222. https://doi.org/10.1016/j.ijpsycho.2003.09.005

Richards, J. E. (2003). Cortical sources of event-related potentials in the prosaccade and antisaccade task. *Psychophysiology*, *40*(6), 878–894. https://doi.org/10.1111/1469-8986.00106

Riemslag, F. C., Van der Heijde, G. L., Van Dongen, M. M., & Ottenhoff, F. (1988). On the origin of the presaccadic spike potential. *Electroencephalography and Clinical Neurophysiology*, *70*(4), 281–287. https://doi.org/10.1016/0013-4694(88)90046-6

Riggs, L. A., Merton, P. A., & Morton, H. B. (1974). Suppression of visual phosphenes during saccadic eye movements. *Vision Research*, *14*(10), 997–1011. https://doi.org/10.1016/0042-6989(74)90169-2

Rodionov, V., Elidan, J., & Sohmer, H. (1996). Analysis of the middle latency evoked potentials to angular acceleration impulses in man. *Electroencephalography and Clinical Neurophysiology*, *100*(4), 354–361. https://doi.org/10.1016/0168-5597(96)95515-X

Rottach, K. G., Das, V. E., Wohlgemuth, W., Zivotofsky, A. Z., & Leigh, R. J. (1998). Properties of Horizontal Saccades Accompanied by Blinks. *Journal of Neurophysiology*, *79*(6), 2895–2902. https://doi.org/10.1152/jn.1998.79.6.2895

Särelä, J., & Vigário, R. (2003). Overlearning in marginal distribution-based ICA: Analysis and solutions. *Journal of Machine Learning Research*, *4*, 1447–1469.

Schall, J. D. (1991). Neuronal activity related to visually guided saccade in the frontal eye fields of rhesus monkeys: Comparison with supplemeantary eye fields. *Journal of Neurophysiology*, *66*(2), 559–579. https://doi.org/10.1152/jn.1991.66.2.559

Schlögl, A., Keinrath, C., Zimmermann, D., Scherer, R., Leeb, R., & Pfurtscheller, G. (2007). A fully automated correction method of EOG artifacts in EEG recordings. *Clinical Neurophysiology*, *118*(1), 98–104. https://doi.org/10.1016/j.clinph.2006.09.003

Schwartzman, D. J., & Kranczioch, C. (2011). In the blink of an eye: The contribution of microsaccadic activity to the induced gamma band response. *International Journal of Psychophysiology*, *79*(1), 73–82. https://doi.org/10.1016/j.ijpsycho.2010.10.006

Semlitsch, H. V., Anderer, P., Schuster, P., & Presslich, O. (1986). A solution for reliable and valid reduction of ocular artifacts, applied to the P300 ERP. *Psychophysiology*, *23*(6), 695–703. https://doi.org/10.1111/j.1469-8986.1986.tb00696.x

Shoker, L., Sanei, S., Wang, W., & Chambers, J. A. (2005). Removal of eye blinking artifact from the electro-encephalogram, incorporating a new constrained blind source

separation algorithm. *Medical and Biological Engineering and Computing*, *43*(2), 290–295. https://doi.org/10.1007/BF02345968

Sun, R., Chan, C., Hsiao, J. H., & Tang, A. C. (2021). Validation of SOBI-DANS method for automatic identification of horizontal and vertical eye movement components from EEG. *Psychophysiology*, *58*(2), e13731. https://doi.org/10.1111/psyp.13731

Thickbroom, G. W., & Mastaglia, F. L. (1985). Presaccadic “spike” potential: Investigation of topography and source. *Brain Research*, *339*(2), 271–280. https://doi.org/10.1016/0006-8993(85)90092-7

Thickbroom, G. W., & Mastaglia, F. L. (1986). Presaccadic spike potential. Relation to eye movement direction. *Electroencephalography and Clinical Neurophysiology*, *64*(3), 211–214. https://doi.org/10.1016/0013-4694(86)90167-7

Trujillo, L. T., Peterson, M. A., Kaszniak, A. W., & Allen, J. J. (2005). EEG phase synchrony differences across visual perception conditions may depend on recording and analysis methods. *Clinical Neurophysiology*, *116*(1), 172–189. https://doi.org/10.1016/j.clinph.2004.07.025

Tsutsui, J., Ohnishi, T., Fukai, S., & Matsuda, E. (1987). Moving topography of human presaccadic spike potentials in visually triggered saccade and optokinetic nystagmus. *Japanese Journal of Ophthalmology*, *31*(3), 489–500.

Urigüen, J. A., & Garcia-Zapirain, B. (2015). EEG artifact removal—State-of-the-art and guidelines. *Journal of Neural Engineering*, *12*(3), 031001. https://doi.org/10.1088/1741-2560/12/3/031001

Verleger, R. (1991). The instruction to refrain from blinking affects auditory P3 and N1 amplitudes. *Electroencephalography and Clinical Neurophysiology*, *78*(3), 240–251. https://doi.org/10.1016/0013-4694(91)90039-7

Viola, F., Thorne, J., Edmonds, B., Schneider, T., Eichele, T., & Debener, S. (2009). Semi-automatic identification of independent components representing EEG artifact. *Clinical Neurophysiology*, *120*(5), 868–877. https://doi.org/10.1016/j.clinph.2009.01.015

Wallstrom, G. L., Kass, R. E., Miller, A., Cohn, J. F., & Fox, N. A. (2004). Automatic correction of ocular artifacts in the EEG: a comparison of regression-based and component-based methods. *International Journal of Psychophysiology*, *53*(2), 105–119. https://doi.org/10.1016/j.ijpsycho.2004.03.007

Weinstein, J. M., & Balaban, C. D. (1984). The pre-saccadic evoked potential: Normative data and clinical studies. *Proc. Neuro-Ophthal. INOS Fifth Meeting*, 149–154.

Weinstein, J. M., Balaban, C. D., & VerHoeve, J. N. (1991). Directional tuning of the human presaccadic spike potential. *Brain Research*, *543*(2), 243–250. https://doi.org/10.1016/0006-8993(91)90034-S

Winkler, I., Haufe, S., & Tangermann, M. (2011). Automatic Classification of Artifactual ICA-Components for Artifact Removal in EEG Signals. *Behavioral and Brain Functions*, *7*(1), 30. https://doi.org/10.1186/1744-9081-7-30

Yuval-Greenberg, S., Tomer, O., Keren, A. S., Nelken, I., & Deouell, L. Y. (2008). Transient induced gamma-band response in EEG as a manifestation of miniature saccades. *Neuron*, *58*(3), 429–441. https://doi.org/10.1016/j.neuron.2008.03.027

Zeng, H., Song, A., Yan, R., & Qin, H. (2013). EOG Artifact Correction from EEG Recording Using Stationary Subspace Analysis and Empirical Mode Decomposition. *Sensors*, *13*(11), 14839–14859. https://doi.org/10.3390/s131114839

Zhou, W., & Gotman, J. (2009). Automatic removal of eye movement artifacts from the EEG using ICA and the dipole model. *Progress in Natural Science*, *19*(9), 1165–1170. https://doi.org/10.1016/j.pnsc.2008.11.013